JACS
JOURNAL OF THE AMERICAN CHEMICAL SOCIETY

Article

pubs.acs.org/JACS

Recognition Characteristics of an Adaptive Vesicular Assembly of Amphiphilic Baskets for Selective Detection and Mitigation of Toxic Nerve Agents

Shigui Chen, Yian Ruan, Jason D. Brown, Christopher M. Hadad, and Jovica D. Badjić*

Department of Chemistry and Biochemistry, The Ohio State University, 100 West 18th Avenue, Columbus, Ohio 43210, United States

Supporting Information

ABSTRACT: We used isothermal titration calorimetry to investigate the affinity of basket **1** (470 Å^3) for trapping variously sized and shaped organophosphonates (OPs) **2**−**12** (137−244 Å^3) in water at 298.0 K. The encapsulation is, in each case, driven by favorable entropy ($T\Delta S°$ = 2.9 kcal/mol), while the enthalpic component stays small and in some cases endothermic ($\Delta H° \geq -1$ kcal/mol). Presumably, a desolvation of basket **1** and OP guests permits the inclusion complexation at room temperature via a "classical" hydrophobic effect. The amphiphilic basket **1** shows a greater affinity ($\Delta G° \approx -5$ to -6 kcal/mol), both experimentally and computationally, for encapsulating larger organophosphonates whose size and shape correspond to VX-type agents (289 A^3). Importantly, baskets assemble into a vesicular nanomaterial ($D_H \approx 350$ nm) that in the presence of neutral OP compounds undergoes a phase transition to give nanoparticles ($D_H \approx 250$ nm). Upon the addition of an anionic guest to basket **1**, however, there was no formation of nanoparticles and the vesicles grew into larger vesicles ($D_H \approx 750$ nm). The interconversion of the different nanostructures is reversible and, moreover, a function of the organophosphonate present in solution. On the basis of ^{1}H NMR spectroscopic data, we deduced that neutral guests insert deep into the basket's cavity to change its shape and thereby promote the conversion of vesicles into nanoparticles. On the contrary, the anionic guests reside at the northern portion of the host to slightly affect its shape and geometric properties, thereby resulting in the vesicles merely transforming into larger vesicles.

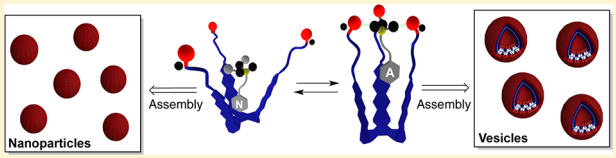

In spite of the Chemical Weapons Convention (CWC) of 1993 forbidding the production and stockpiling of nerve agents, these toxic substances remain to pose a great threat to civilians and/or military personnel around the world.[1] Nerve agents of the G and V types are tetrahedral organophosphorus compounds that were developed in the first half of the past century.[2] These compounds act as powerful inhibitors of acetylcholinesterase (AChE) in the synapses of both humans and animals.[3] As a result of their size (130−290 Å^3),[4] shape, and chemical reactivity,[5] nerve agents occupy the active site of AChE whereby they react with the nucleophilic serine residue of the catalytic triad.[6] The covalent enzyme inhibition causes an accumulation of the acetylcholine neurotransmitter and hyperactivity of cholinergic nerves, muscles, and glands to eventually result in asphyxiation and death.[3a,7] Indeed, U.S. military personnel are equipped with kits (containing atropine, diazepam, and pralidoxime)[8] to treat the effects of poisoning, yet there is a need for developing more effective prophylactic measures[9] in addition to improving ways for completing a rapid removal[3c,10] as well as unambiguous identification of minute quantities of these toxic substances.[11] We reason that functionalized concave compounds (cavitands)[11a,f,12] could be designed and then prepared in the laboratory so that they are complementary to nerve agents and capable of their selective complexation, isolation, and degradation.[13] By developing ways for the effective trapping of the organophosphorus compounds with an artificial host,[14] one could facilitate their rapid degradation[10d,15] and/or removal from the environment.[13b,14,16] In this vein, we recently discovered[17] that amphiphilic baskets of type **1** (V = 477 Å^3, Figure 1) assemble in water (0.5−5.0 mM) to form large unilamellar vesicles (∼350 nm in diameter).[18] The vesicular membrane (∼4 nm) consists of pairs of truncated-cone-like baskets that, we posit, pack[19] such that their hydrophobic cup-shaped components populate the interior of the bilayer while the peripheral and

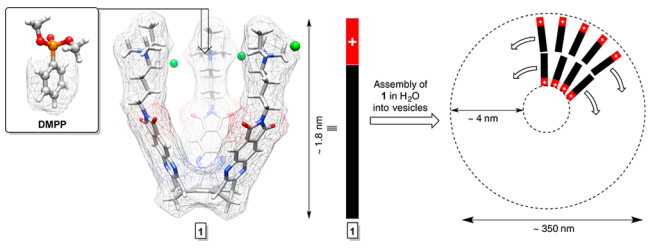

Figure 1. Left: energy-minimized structure of basket **1** (MMFFs, Spartan) and DMPP guest. Right: the basket is an amphiphilic molecule that in water assembles into large unilamellar vesicles capable of complexing DMPP.

Received: October 11, 2014
Published: November 17, 2014

   dx.doi.org/10.1021/ja510477q | J. Am. Chem. Soc. 2014, 136, 17337−17342

polar ammonium groups face the aqueous solvent. Upon complexing dimethyl phenylphosphonate (DMPP has a volume of 184 Å^3 and is therefore similar in size to soman, 186 Å^3), the vesicles turn into nanoparticles (~200 nm in diameter) lacking the water reservoir and, presumably, containing baskets packed into multilayers. On the basis of ^{1}H NMR spectroscopic results, we hypothesized that a change in the shape of baskets holding DMPP in their cavity contributed to the observed phase transition of the nanomaterial. In particular, the tetrahedral DMPP guest occupies C_3-symmetric **1** by positioning its phenyl moiety into the cavity and thereby causing its expansion while keeping the three remaining groups at the basket's rim (Figure 1). The original investigation prompted a number of intriguing questions. Will assembled baskets of type **1** complex other organophosphonates (OPs) in water? What is the nature of such host–guest interactions? Does the vesicle–nanoparticle phase transition take place upon the inclusion complexation of guests other than DMPP? To address these questions, pertaining to a potential application of the vesicular material for detection and mitigation of tetrahedral nerve agents (132–289 Å^3),[13a,20] we set to investigate the entrapment of 11 organophosphonates varying in size (137–244 Å^3), shape, and also formal charge with C_3-symmetric and amphiphilic **1** in water.

RESULTS AND DISCUSSION

Organophosphonates **2**–**5** were chosen to carry an aliphatic R moiety that is, in each case, spherical yet varies in size (137–244 Å^3) and hydrophobicity (Figure 2). As the volume of the host's concave cavity is estimated to be 470 Å^3,[17] we reasoned that larger guests should populate the basket's inner space to a greater extent.[21] That is to say, OPs **2**–**5** could, along the series, exhibit a greater complementarity[22] to **1** and thereby possess a progressively higher affinity for populating its inner space.

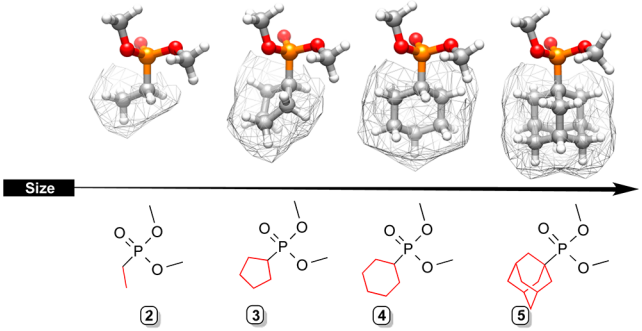

	2	3	4	5
Size (Å^3)	137	180	197	244
K_a (M^{-1}) 10^3	0.26±0.02	0.34±0.08	2.1±0.5	4.6±0.2
$\Delta H°$ (kcal/mol)	−0.08±0.01	−0.54±0.08	−0.50±0.04	−0.27±0.03
$-T\Delta S°$ (kcal/mol)	−3.21±0.05	−2.90±0.16	−4.03±0.15	−4.72±0.04
$\Delta G°$ (kcal/mol)	−3.29±0.05	−3.44±0.14	−4.53±0.14	−4.99±0.02

Figure 2. Energy-minimized structures of progressively bigger organophosphonates **2**–**5** (MMFFs, Spartan), each carrying an aliphatic group. The inclusion complexation of these compounds and basket **1** (1.0 mM) was studied with ITC (298.0 K) in H_2O to, in each case, provide thermodynamic parameters pertaining to the formation of a 1:1 complex.

With the assistance of isothermal titration calorimetry (ITC; Figure 2),[23] we obtained thermodynamic parameters for the inclusion of **2**–**5** in basket **1** in water at 298.0 K (Figures S1–S11, Supporting Information). As originally anticipated, the standard free energy ($\Delta G°$, Figure 2) for the formation of 1:1 complexes decreases in the series, with dimethyl ethylphosphonate **2** having the lowest affinity (K_a = 260 M^{-1}, Figure 2) and dimethyl adamantylphosphonate **5** having the highest affinity (K_a = 4.6 × 10^3 M^{-1}, Figure 2) for occupying the amphiphilic **1**. Importantly, the host–guest stoichiometry coefficient n was, in each curve-fitting, fixed to 1 (Figures S1–S11). While the host–guest complementarity increases from **2** to **5**, the interaction enthalpy remains rather small and invariant ($\Delta H°$ = −0.08 to −0.54 kcal/mol, Figure 2). In fact, the experimentally determined entropy of the interaction increases ($-T\Delta S°$ = −2.90 to −4.72 kcal/mol, Figure 2) and for the most part (>80%) contributes to the overall free energy of the complexation ($\Delta G°$). It follows that the formation of [**1**⊂**2**–**5**] is, at room temperature, promoted via a "classical" hydrophobic effect[24] whereby the "release" of water molecules from hydrophobic surfaces of "free" basket **1** and guests **2**–**5** drives the inclusion complexation: the larger the hydrophobic surface area, the greater the number of water molecules released (greater $\Delta S°$) and the stronger the intermolecular interaction (lower $\Delta G°$, Figure 2)![25] Clearly, basket **1** prefers to trap larger OP compounds and could perhaps hold even more sizable and hydrophobic V-type agents (>280 Å^3)[4] in its interior.

Compounds **6**–**9** encompass an aromatic P–R moiety, with a benzene ring linked to the central phosphorus by a hydrocarbon chain (Figure 3). In particular, a single methylene group in **7** twists the phenyl ring with respect to the $(CH_3O)_2P{=}O$ unit (Figure 3). In the case of the three remaining guests (**6**, **8**, **9**), however, the R group is almost orthogonal with reference to the top part of the molecule (Figure 3). On the basis of the geometry of the guests, we surmised that **6**, **8**, and **9** should be more complementary[26] than **7** to the truncated-cone-like interior of **1** (see below, but also Figure 1). The experimental enthalpy (ITC, Figure 2) of the interaction was indeed least favorable for **7** ($\Delta H°$ = −0.46 kcal/mol) and more exothermic ($\Delta H°$ < −1.0 kcal/mol) for the other three guests, all in agreement with the host–guest complementarity argument. Apparently, compounds **6**, **8**, and **9**

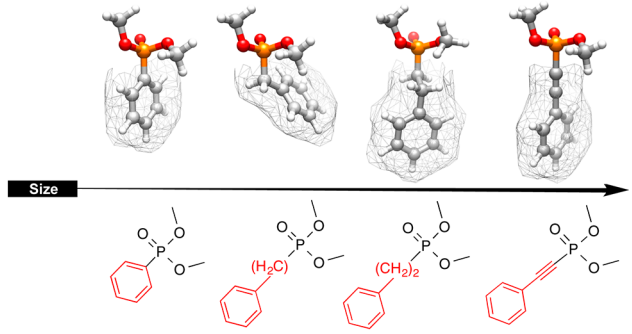

	6	7	8	9
Size (Å^3)	184	203	221	214
K_a (M^{-1}) 10^3	2.0±0.5	0.36±0.03	1.19±0.09	6.04±0.14
$\Delta H°$ (kcal/mol)	−1.06±0.03	−0.46±0.07	−1.10±0.03	−1.29±0.04
$-T\Delta S°$ (kcal/mol)	−3.44±0.14	−3.03±0.09	−3.09±0.05	−3.87±0.04
$\Delta G°$ (kcal/mol)	−4.50±0.15	−3.49±0.05	−4.19±0.04	−5.16±0.01

Figure 3. Energy-minimized structures of organophosphonates **6**–**9** (MMFFs, Spartan) carrying different aromatic groups. The inclusion complexation of these compounds and basket **1** (1.0 mM) was studied with ITC (298.0 K) in H_2O to, in each case, provide thermodynamic parameters pertaining to the formation of a 1:1 complex.

dx.doi.org/10.1021/ja510477q | J. Am. Chem. Soc. 2014, 136, 17337–17342

carrying aromatic residues form stronger noncovalent contacts ($\Delta H^\circ \leq -0.5$ kcal/mol, Figure 3) and **2**–**5** comprising aliphatic groups ($\Delta H^\circ \geq -0.5$ kcal/mol, Figure 2) form weaker noncovalent contacts with basket **1**. Perhaps, noncovalent interactions of the π–π type,[27] in the case of **6**, **8**, and **9** as guests interacting with host **1**, give rise to stronger intermolecular forces than the C–H···π contacts[28] available with guests **2**–**5**. In general, more sizable guests, from both series, form stronger 1:1 complexes with the basket, albeit there is a smaller span in the volumes along **6**–**9** (180–220 Å^3). Finally, the entropic contribution ($-T\Delta S^\circ$ = −3.03 to −3.87 kcal/mol, Figure 3) dominates the standard free energy ΔG° of the complexations, again indicating that the hydrophobic effect drives the observed encapsulations;[24,25] note that our preliminary data suggest a negative change in the heat capacity ($\Delta C_p < 0$) of the complexation, which is in line with a hydrophobically driven association.

The conformational characteristics of basket **1** were examined with a Monte Carlo computational algorithm (AMBER) followed by a series of molecular dynamics (MD) simulations in water.[4,29] A clustering analysis of the resulting MD results gave 10 structures representing the conformational characteristics of **1** (Figure 4A). Evidently, the amphiphilic **1** is

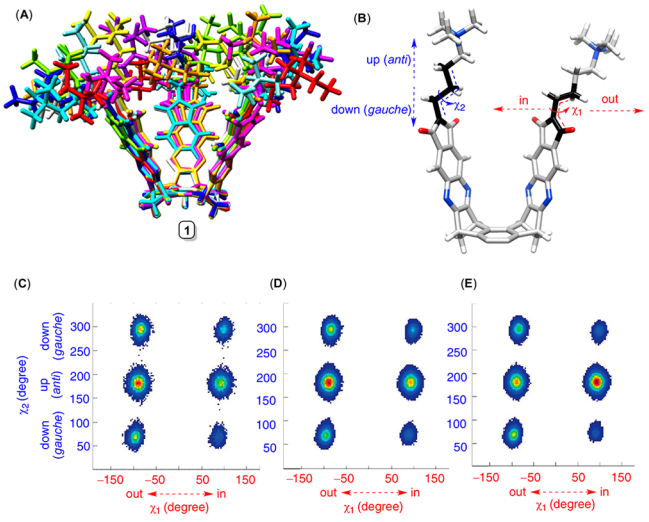

Figure 4. (A) Ten representative conformers of basket **1** were identified from an MD (AMBER) study in H_2O followed by clustering analysis of the computed MD trajectories via the RMSD protocol and using the ptraj module of AMBER. (B) Two torsions, χ_1 (red, in/out) and χ_2 (blue, up/down), describe the position of three alkyl chains in **1**. The contour plots depict a computed conformational distribution of **1** (C), [**1**–**6**] (D), and [**1**–**8**] (E) in water (MD, AMBER). In the third dimension, white designates absence of conformational states, while red corresponds to the highest population of conformational states.

preorganized[30] for complexing guests with three aliphatic chains at the rim extending into the water solution to create a "hydrophobic pocket". Alternatively, a survey of all MD conformations of **1** provides a three-dimensional map of its conformational characteristics with two torsional degrees of freedom, χ_1 (in/out, Figure 4B) and χ_2 (up/down, Figure 4B), describing the position of the aliphatic chains with respect to the cup-shaped platform. Apparently, there is an abundance of out/up rotamers (Figure 4C) accompanied by a smaller population of out/down structures. Likewise, we completed the MD conformational analysis of [**1**–**6**] (Figure 4D) and [**1**–**8**] (Figure 4E) host–guest complexes situated in the host while solvated by explicit water. Importantly, the conformational characteristics of the [**1**⊂guest] complexes resemble those of the free basket **1** (Figure 4B).

In particular, the conformation of the host's aliphatic chains is altered to a small degree upon complexation.[31] With a guest molecule inside the host, the hydrophobic chains adopt in/up orientations (Figure 4C–E) to, perhaps, interact with the OP guest. Finally, the results from molecular docking (Autodock 4.0) of increasingly bigger guests (**2**, **4**, **6**, **7**, **8**) into basket **1** revealed that the percentage of entrapped structures increases along the series (Table S1, Supporting Information), thereby supporting our experimental findings (Figures 2 and 3).

In addition, we used calorimetry to investigate the complexation of dianionic compounds **10**–**12** and tricationic **1** in H_2O and 298.0 K (Figure 5); note that compound **13** is chemically

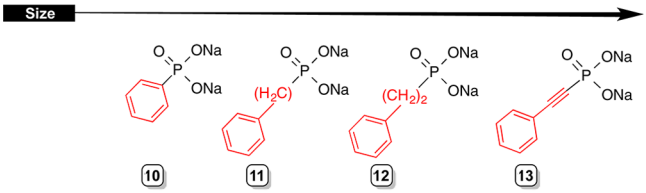

	10	**11**	**12**	**13**
Size (Å^3)	138	157	175	167
K_a (M^{-1}) 10^4	0.28±0.04	0.59±0.08	6.61±0.02	——
ΔH° (kcal/mol)	+2.75±0.16	+4.49±0.14	+4.54±0.17	——
$-T\Delta S^\circ$ (kcal/mol)	−7.45±0.18	−9.63±0.16	−11.11±0.07	——
ΔG° (kcal/mol)	−4.70±0.08	−5.14±0.08	−6.57±0.01	——

Figure 5. Chemical structures of dianionic organophosphonates **10**–**13** (MMFFs, Spartan) carrying different aromatic groups. The inclusion complexation of **10**–**12** and basket **1** (1.0 mM) was studied with ITC (298.0 K) in H_2O to, in each case, provide thermodynamic parameters pertaining to the formation of a 1:1 complex; note that compound **13** is chemically unstable at a low pH, and we were unable to obtain it in its pure form for completing the experimental measurements.

unstable, undergoing a rapid decomposition in water. The dianionic OPs carry negative charges that are complementary to the positive ammonium groups at the periphery of basket **1**. Interestingly, the formation of [**1**⊂**10**], [**1**⊂**11**], and [**1**⊂**12**] complexes was endothermic (ΔH° > 2.5 kcal/mol, Figure 5), with entropy being the dominant contribution to the complexations at room temperature ($-T\Delta S^\circ \ll -7.5$ kcal/mol, Figure 5). As both tetraalkylammonium and phosphonate groups are effectively solvated in water,[32] we reason that the observed endothermic complexations are due to energy-demanding desolvation of the charged host **1** and guests **10**–**12** at room temperature![33] The release of the solvent molecules, as in the case of neutral guests, drives the complexation with larger anionic organophosphonates possessing a greater affinity toward **1**.[34] Interestingly, the standard free energies for the encapsulation of anionic guests (ΔG°, Figure 5) are more exergonic than those corresponding to the neutral ones (Figures 2 and 3).

The addition of neutral guest **8** (20.0 mM) to host **1** (1.0 mM), assembled into vesicles (Figure 6), gave rise to the inclusion complex [**1**⊂**8**], which aggregated into nanoparticles for which the size distribution (PDI (polydispersity index) = 0.56) is centered at $D_H \approx 250$ nm as measured by dynamic light scattering (DLS; Figure 6). Upon the addition of anionic guest

dx.doi.org/10.1021/ja510477q | J. Am. Chem. Soc. 2014, 136, 17337–17342

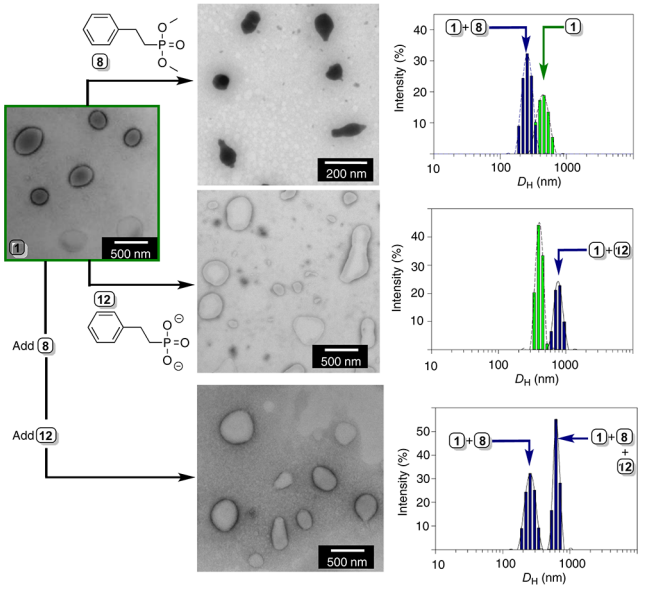

Figure 6. Left: TEM image of amphiphilic **1** (1.0 mM in H_2O). Top: TEM image of amphiphilic **1** (1.0 mM in H_2O) containing **8** (20.0 mM) and a plot showing the size distribution of the assembled particles in a solution of **1** (1.0 mM in H_2O, green) and **1** (1.0 mM in H_2O) containing compound **8** (20.0 mM, blue) as examined with DLS at 298.0 K. Middle: TEM image of a solution of **1** (1.0 mM in H_2O) containing **12** (20.0 mM) and a plot showing the size distribution of the assembled particles in a solution of **1** (1.0 mM in H_2O, green) and **1** (1.0 mM in H_2O) containing compound **12** (20.0 mM, blue) as examined with DLS at 298.0 K. Bottom: TEM image of a solution of **1** (1.0 mM in H_2O) obtained after a successive addition of **8** (20.0 mM) and **12** (20.0 mM) and a plot showing the size distribution of the assembled particles in a solution of **1** (1.0 mM in H_2O) after a successive addition of **8** (20.0 mM, left) and **12** (20.0 mM, right) as examined with DLS at 298.0 K. All TEM images were obtained by deposition of each solution on a copper grid and staining it with uranyl acetate.

12 (20.0 mM) to basket **1** (1.0 mM), however, the formation of nanoparticles was not observed; instead, the vesicles, consisting of basket **1**, grew into larger vesicles comprising [**1**⊂**12**] complexes ($D_H \approx 750$ nm with PDI = 0.41, Figure 6)! The membrane of the newly formed unilamellar vesicles (transmission electron microcopy (TEM), Figure S12, Supporting Information) is estimated to be 4.0 nm and therefore composed of pairs of [**1**⊂**12**] (each ∼2 nm, Figure 1) packed into a double layer. Finally, when nanoparticles containing closely assembled [**1**⊂**8**] (20 mM) were exposed to anionic guest **12** (20.0 mM), the formation of [**1**⊂**12**] ensued with the transformation of nanoparticles back into vesicles ($D_H \approx 750$ nm, Figure 6)! Evidently, the self-assembled nanomaterial[35] comprising basket **1** or [**1**⊂guest] complexes is dynamic with adaptive and reversible characteristics.[36] That is to say, the material alters its shape and size in response to the organophosphonate substance in its surroundings.[37] Since the complex [**1**⊂**8**] containing a neutral OP formed nanoparticles (Figure 6), while [**1**⊂**12**] comprising an anionic OP gave larger vesicles (Figure 6), we pondered whether the formal charge of each guest within [**1**⊂guest] complexes could have an effect on the mode of the aggregation of such complexes in water. To investigate this point of view, we turned to ^{1}H NMR spectroscopy. ^{1}H NMR study (500 MHz, 298.0 K) of an incremental addition of **8** and **12** to a D_2O solution of vesicular **1** revealed a perturbation of the magnetic environment of the proton nuclei of both the host and guests (Figures S13 and S14, Supporting Information). In particular, the nonlinear least-squares analysis of the chemical shift of the host's H_a signal (Figure 7A, 1:1 stoichiometric model) gave $K_a = (1.12 \pm 0.09) \times 10^3$ M^{-1} ($R^2 = 0.99$, Figure 7B) for the formation of [**1**⊂**8**];[38] note that this result is in excellent agreement with our calorimetric data (Figure 3). The broadening of ^{1}H NMR signals corresponding to basket **1** in D_2O (Figure S13) is allegedly due to the unique dynamic characteristics of this host being organized into vesicles.[17] The formation of the [**1**⊂**8**] complex, however, is accompanied by a sharpening of the ^{1}H NMR resonances,[17] yet the signal broadening remained in the case of [**1**−**12**] (Figures S14)! This result bodes well with our finding that vesicular **1** would in the presence of neutral **8** change into nanoparticles while retaining its vesicular form after complexing the anionic **12**; note that, due to the extensive broadening of the host's ^{1}H NMR resonances, we were unable to use NMR spectroscopy for quantifying the binding affinity (K_a) of **12** toward **1**. Following, we constructed a plot showing the normalized change ($\Delta\delta = \delta_{obsd} - \delta_{bound}$) in the observed chemical shifts of the ^{1}H NMR signals of **8** (Figure 7C) and **12** (Figure 7D) as a function of their increasing concentration in the solution of **1** (1.0 mM in D_2O). Since the ^{1}H NMR signals of both guests showed an upfield shift, upon complexing the host, we reasoned that (as in the case of DMPP, Figure 1)[17] both **8** and **12** occupy the inner space of **1**. That is to say, the guests should reside in the shielded region of the aromatic cup-

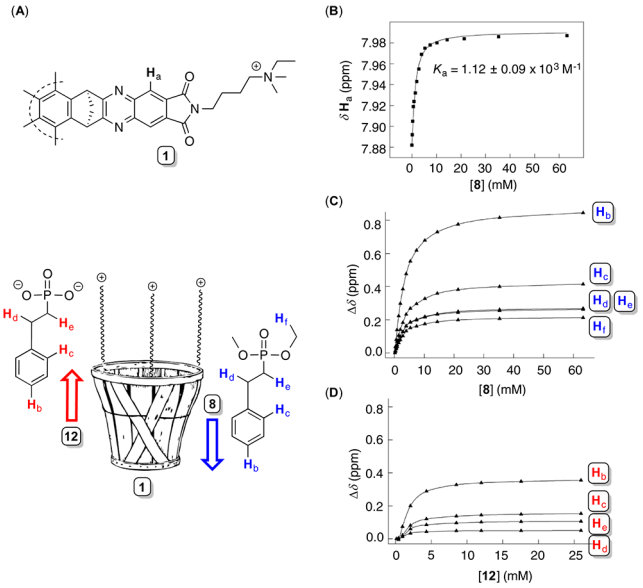

Figure 7. (A) Chemical structure of basket **1** (top) and its schematic representation with compounds **8** and **12** (bottom). (B) The nonlinear least-squares analysis of the ^{1}H NMR spectroscopic data, corresponding to the formation of [**1**⊂**8**], provided $K_a = (1.12 \pm 0.01) \times 10^3$ M^{-1} ($R^2 = 0.99$); the data were obtained upon an incremental addition of **8** (0−60 mol equiv) to a solution of **1** (1.0 mM in D_2O) and monitored with ^{1}H NMR spectroscopy (400 MHz; Figure S13, Supporting Information) at 298.0 K. (C) Normalized ^{1}H NMR chemical shifts ($\Delta\delta = \delta_{obsd} - \delta_{bound}$) of H_b−H_f protons in **8** (blue) as a function of the overall concentration of this guest titrated to a 1.0 mM solution of **1** in D_2O. (D) Normalized ^{1}H NMR chemical shifts ($\Delta\delta = \delta_{obsd} - \delta_{bound}$) of H_b−H_e protons in **12** (red) as a function of the overall concentration of this guest titrated to a 1.0 mM solution of **1** in D_2O.

dx.doi.org/10.1021/ja510477q | J. Am. Chem. Soc. 2014, 136, 17337−17342

shaped platform of **1** for their protons to "experience" a weaker magnetic field. A greater perturbation of the magnetic environments of the aromatic $H_{b/c}$ than aliphatic $H_{d/e/f}$ nuclei (Figure 7C/D), however, suggests that the benzene moiety of **8** and **12** inhabits the cavity of **1** with methoxy/ethyl groups residing at the northern region of the host (Figure 7A). Finally, the chemical shift of the benzene H_b proton is in neutral **8** ($\Delta\delta \approx 0.8$ ppm, Figure 7C) affected to a much greater degree than in anionic **12** ($\Delta\delta \approx 0.4$ ppm, Figure 7D). Since both guests occupy basket **1**, with their benzene ring inserted into the cavity, we deduce that the H_b nucleus is more shielded when positioned deeper within **1** and thereby closer to its aromatic "floor" (Figure 7A). It follows that neutral **8** penetrates the concave host more than anionic **12**! This conclusion is, perhaps, further supported by the notion that two negatively charged oxygen atoms of the anionic **12** are likely to position near the positively charged ammonium groups in **1**, thereby situating the entire guest molecule in the northern region of the complex (Figure 7A). Indeed, the energy-minimized structures of [**1**⊂**8**] and [**1**⊂**12**] (MMFFs, Figure 8) show that guest **12** resides in the cavity of **1** with a H_b centroid distance of 5.26 Å (Figure 8), while organophosphonate **8** is more deeply inserted into **1** with a H_b centroid distance of only 4.01 Å. As a consequence of such different encapsulation geometries, the more populated basket [**1**⊂**8**] expands its side arms to a greater degree with an average N···N distance of 9.07 Å, while the gap remains 8.45 Å for [**1**⊂**12**] (Figure 8). Since the binding of neutral guest **8** causes a greater change in the shape of **1**, we postulate that the packing of vesicular **1** must also be affected to a greater degree to prompt the [**1**⊂**8**] complex to assemble into nanoparticles.[17] Upon trapping the anionic **12**, however, basket **1** turns into the similarly shaped [**1**⊂**12**] so that the vesicular nanomaterial merely reorganizes into more sizable vesicles with the critical packing parameter P remaining at ~0.5−1.[19]

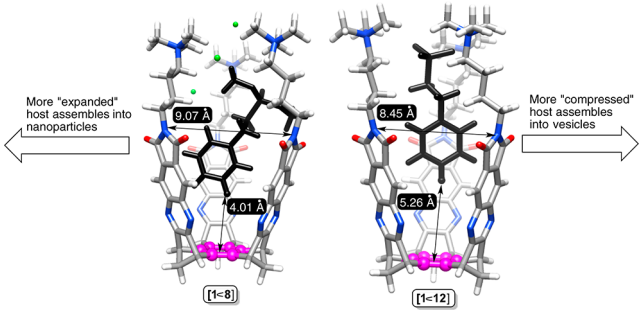

Figure 8. Energy-minimized structures of [**1**⊂**8**] and [**1**⊂**12**] (MMFFs, Spartan) showing different positions of neutral guest **8** and anionic **12** in the interior of cationic **1**. A different population of the basket's inner space affects the shape of this amphiphilic host and allegedly its assembly characteristics.

CONCLUSIONS

The unambiguous detection, removal, and rapid degradation of nerve agents (132−289 Å^3) can, perhaps, be accomplished with functionalized artificial cavitands capable of selectively encapsulating these toxic substances. We hereby demonstrate how C_3-symmetric baskets of type **1** (V = 477 Å^3) possess an affinity (in the millimolar range) for trapping larger organophosphonates whose size and shape correspond to soman (~186 Å^3) and/or V-type agents (>289 Å^3); the apparent affinity could be useful for promoting the hydrolysis of nerve agents but is still low for the effective removal of these substances from the environment via entrapment. Markedly, the encapsulation in aqueous environments is driven by favorable entropy ($\Delta S^\circ > 0$) whereby the desolvation of basket **1** and OP guests permits the encapsulation via a classical hydrophobic effect. Importantly, baskets assemble into vesicular nanomaterial that in the presence of OP compounds undergoes a phase transition to give nanoparticles or larger vesicles depending on the nature of the guest. Thus, with neutral guests capable of inserting deeper into the basket's cavity, to affect its shape, the vesicles change into nanoparticles. On the contrary, with anionic guests residing at the northern portion of the baskets, thereby slightly affecting their shape, the vesicles merely transform into larger vesicles. A change in the shape of host−guest complexes, as a function of the guest's complementarity to the host, is thus manifested at the nanosized level to give rise to a particular type of dynamic material.[39] Notably, our discovery that vesicular **1** reversibly changes its form in the presence of OPs may, perhaps, be applied for detecting and removing nerve agents. We are currently working on examining the potential of such an intriguing proposition.

ASSOCIATED CONTENT

Supporting Information

Additional details of the experimental and computational protocols. This material is available free of charge via the Internet at http://pubs.acs.org.

AUTHOR INFORMATION

Corresponding Author

badjic@chemistry.ohio-state.edu

Notes

The authors declare no competing financial interest.

ACKNOWLEDGMENTS

This work was financially supported with funds obtained from the Department of Defense, Defense Threat Reduction Agency (Grant HDTRA1-11-1-0042). Computational support from the Ohio Supercomputer Center is gratefully acknowledged.

REFERENCES

(1) Mika, O. J.; Fiserova, L. *Toxin Rev.* **2011**, *30*, 115−121.
(2) Kim, K.; Tsay, O. G.; Atwood, D. A.; Churchill, D. G. *Chem. Rev.* **2011**, *111*, 5345−5403.
(3) (a) Bajgar, J.; Kuca, K.; Jun, D.; Bartosova, L.; Fusek, J. *Curr. Drug Metab.* **2007**, *8*, 803−809. (b) Hoernberg, A.; Tunemalm, A.-K.; Ekstroem, F. *Biochemistry* **2007**, *46*, 4815−4825. (c) Mercey, G.; Verdelet, T.; Renou, J.; Kliachyna, M.; Baati, R.; Nachon, F.; Jean, L.; Renard, P.-Y. *Acc. Chem. Res.* **2012**, *45*, 756−766.
(4) Ruan, Y.; Taha, H. A.; Yoder, R. J.; Maslak, V.; Hadad, C. M.; Badjic, J. D. *J. Phys. Chem. B* **2013**, *117*, 3240−3249.
(5) Creasy, W. R.; Fry, R. A.; McGarvey, D. J. *J. Phys. Chem. A* **2012**, *116*, 7279−7286.
(6) Ekstrom, F.; Hornberg, A.; Artursson, E.; Hammarstrom, L.-G.; Schneider, G.; Pang, Y.-P. *PLoS One* **2009**, *4*, e5957.
(7) Spradling, K. D.; Dillman, J. F. *Adv. Mol. Toxicol.* **2011**, 111−144.
(8) Dolgin, E. *Nat. Med.* **2013**, *19*, 1194−1195.
(9) (a) Dwyer, M.; Javor, S.; Ryan, D. A.; Smith, E. M.; Wang, B.; Zhang, J.; Cashman, J. R. *Biochemistry* **2014**, *53*, 4476−4487. (b) Nachon, F.; Brazzolotto, X.; Trovaslet, M.; Masson, P. *Chem.-Biol. Interact.* **2013**, *206*, 536−544. (c) Sit, R. K.; Fokin, V. V.; Amitai, G.; Sharpless, K. B.; Taylor, P.; Radic, Z. *J. Med. Chem.* **2014**, *57*, 1378−1389. (d) Otto, T. C.; Scott, J. R.; Kauffman, M. A.; Hodgins, S. M.; diTargiani, R. C.; Hughes, J. H.; Sarricks, E. P.; Saturday, G. A.;

Hamilton, T. A.; Cerasoli, D. M. *Chem.-Biol. Interact.* **2013**, *203*, 186−190. (e) De Coste, J. B.; Peterson, G. W. *Chem. Rev.* **2014**, *114*, 5695−5727.
(10) (a) Prasad, G. K. *Nanotechnol. Environ. Decontam.* **2011**, 193−236. (b) Kang, B.; Kurutz, J. W.; Youm, K.-T.; Totten, R. K.; Hupp, J. T.; Nguyen, S. B. T. *Chem. Sci.* **2012**, *3*, 1938−1944. (c) Smith, B. M. *Chem. Soc. Rev.* **2008**, *37*, 470−478. (d) Raushel, F. M. *Nature* **2011**, *469*, 310−311.
(11) (a) Ajami, D.; Rebek, J. *Org. Biomol. Chem.* **2013**, *11*, 3936−3942. (b) Wallace, K. J.; Fagbemi, R. I.; Folmer-Andersen, F. J.; Morey, J.; Lynth, V. M.; Anslyn, E. V. *Chem. Commun.* **2006**, 3886−3888. (c) Dale, T. J.; Rebek, J., Jr. *J. Am. Chem. Soc.* **2006**, *128*, 4500−4501. (d) Ordronneau, L.; Carella, A.; Pohanka, M.; Simonato, J. P. *Chem. Commun.* **2013**, *49*, 8946−8948. (e) Hiscock, J. R.; Piana, F.; Sambrook, M. R.; Wells, N. J.; Clark, A. J.; Vincent, J. C.; Busschaert, N.; Brown, R. C. D.; Gale, P. A. *Chem. Commun.* **2013**, *49*, 9119−9121. (f) Tudisco, C.; Betti, P.; Motta, A.; Pinalli, R.; Bombaci, L.; Dalcanale, E.; Condorelli, G. G. *Langmuir* **2012**, *28*, 1782−1789.
(12) (a) Desire, B.; Saint-Andre, S. *Fundam. Appl. Toxicol.* **1986**, *7*, 646−657. (b) Desire, B.; Saint-Andre, S. *Experientia* **1987**, *43*, 395−397. (c) Hennrich, N.; Cramer, F. *J. Am. Chem. Soc.* **1965**, *87*, 1121−1126.
(13) (a) Sambrook, M. R.; Notman, S. *Chem. Soc. Rev.* **2013**, *42*, 9251−9267. (b) Hargrove, A. E.; Nieto, S.; Zhang, T.; Sessler, J. L.; Anslyn, E. V. *Chem. Rev.* **2011**, *111*, 6603−6782.
(14) Borsato, G.; Rebek, J., Jr.; Scarso, A. *Sel. Nanocatal. Nanosci.* **2011**, 105−168.
(15) (a) Barr, L.; Easton, C. J.; Lee, K.; Lincoln, S. F.; Simpson, J. S. *Tetrahedron Lett.* **2002**, *43*, 7797−7800. (b) Hiscock, J. R.; Sambrook, M. R.; Cranwell, P. B.; Watts, P.; Vincent, J. C.; Xuereb, D. J.; Wells, N. J.; Raja, R.; Gale, P. A. *Chem. Commun.* **2014**, *50*, 6217−6220.
(16) (a) Zengerle, M.; Brandhuber, F.; Schneider, C.; Worek, F.; Reiter, G.; Kubik, S. *Beilstein J. Org. Chem.* **2011**, *7*, 1543−1554. (b) Bhowmick, I.; Neelam. *Analyst* **2014**, *139*, 4154−4168.
(17) Chen, S.; Ruan, Y.; Brown, J. D.; Gallucci, J.; Maslak, V.; Hadad, C. M.; Badjic, J. D. *J. Am. Chem. Soc.* **2013**, *135*, 14964−14967.
(18) Voskuhl, J.; Ravoo, B. J. *Chem. Soc. Rev.* **2009**, *38*, 495−505.
(19) (a) Shimizu, T.; Masuda, M.; Minamikawa, H. *Chem. Rev.* **2005**, *105*, 1401−1443. (b) Israelachvili, J. N. *Intermolecular and Surface Forces*; Academic Press: Burlington, MA, 2011.
(20) Ariyadasa, L. W.; Obare, S. O. *Nanotechnol. Environ. Decontam.* **2011**, 347−378.
(21) Ruan, Y.; Wang, B. Y.; Erb, J. M.; Chen, S.; Hadad, C. M.; Badjic, J. D. *Org. Biomol. Chem.* **2013**, *11*, 7667−7675.
(22) Wittenberg, J. B.; Isaacs, L. *Supramol. Chem. Mol. Nanomater.* **2012**, *1*, 25−43.
(23) (a) Schmidtchen, F. P. *Anal. Methods Supramol. Chem.* **2012**, *1*, 67−103. (b) Leavitt, S.; Freire, E. *Curr. Opin. Struct. Biol.* **2001**, *11*, 560−566.
(24) Gibb, B. C. *Chemosensors* **2011**, 3−18.
(25) (a) Chandler, D. *Nature* **2005**, *437*, 640−647. (b) Biedermann, F.; Nau, W. M.; Schneider, H. J. *Angew. Chem., Int. Ed.* **2014**, *53*, 11158−11171.
(26) Cram, D. J., Cram, J. M., Eds. *Container Molecules and Their Guests*; Royal Society of Chemistry: Cambridge, U.K., 1997.
(27) Meyer, E. A.; Castellano, R. K.; Diederich, F. *Angew. Chem., Int. Ed.* **2003**, *42*, 1210−1250.
(28) Ruan, Y.; Peterson, P. W.; Hadad, C. M.; Badjic, J. D. *Chem. Commun.* **2014**, *50*, 9086−9089.
(29) Ruan, Y.; Dalkilic, E.; Peterson, P. W.; Pandit, A.; Dastan, A.; Brown, J. D.; Polen, S. M.; Hadad, C. M.; Badjic, J. D. *Chem.—Eur. J.* **2014**, *20*, 4251−4256.
(30) Faggi, E.; Porcar, R.; Bolte, M.; Luis, S. V.; Garcia-Verdugo, E.; Alfonso, I. *J. Org. Chem.* **2014**, *79*, 9141−9149.
(31) Cram, D. J.; Kaneda, T.; Helgeson, R. C.; Brown, S. B.; Knobler, C. B.; Maverick, E.; Trueblood, K. N. *J. Am. Chem. Soc.* **1985**, *107*, 3645−3657.
(32) Jadhav, V. D.; Schmidtchen, F. P. *Org. Lett.* **2005**, *7*, 3311−3314.
(33) Berger, M.; Schmidtchen, F. P. *Angew. Chem., Int. Ed.* **1998**, *37*, 2694−2696.
(34) (a) Corbellini, F.; Fiammengo, R.; Timmerman, P.; Crego-Calama, M.; Versluis, K.; Heck, A. J. R.; Luyten, I.; Reinhoudt, D. N. *J. Am. Chem. Soc.* **2002**, *124*, 6569−6575. (b) Fochi, F.; Jacopozzi, P.; Wegelius, E.; Rissanen, K.; Cozzini, P.; Marastoni, E.; Fisicaro, E.; Manini, P.; Fokkens, R.; Dalcanale, E. *J. Am. Chem. Soc.* **2001**, *123*, 7539−7552. (c) Rekharsky, M.; Inoue, Y.; Tobey, S.; Metzger, A.; Anslyn, E. *J. Am. Chem. Soc.* **2002**, *124*, 14959−14967.
(35) Philp, D.; Stoddart, J. F. *Angew. Chem., Int. Ed. Engl.* **1996**, *35*, 1155−1196.
(36) Lehn, J.-M. *Top. Curr. Chem.* **2012**, *322*, 1−32.
(37) (a) Rieth, S.; Baddeley, C.; Badjic, J. D. *Soft Matter* **2007**, *3*, 137−154. (b) Hashidzume, A.; Harada, A. *Supramol. Polym. Chem.* **2012**, 231−267. (c) Guo, D.-S.; Wang, K.; Wang, Y.-X.; Liu, Y. *J. Am. Chem. Soc.* **2012**, *134*, 10244−10250.
(38) Hirose, K. *Anal. Methods Supramol. Chem.* **2007**, 17−54.
(39) Aida, T.; Meijer, E. W.; Stupp, S. I. *Science* **2012**, *335*, 813−817.